Chemical Vapor Deposition Growth and Photodetector Performance of Lead-Free All-Inorganic Crystalline $Cs_3Sb_2X_9$ (X=I, Br) Perovskite Thin Films

Sujit Kumer Shil[1,2], Fei Wang[3,4,5], Kingsley O. Egbo[1], Ying Wang[1], Cheuk Kai Gary Kwok[1], Sai-W. Tsang[3], Johnny C. Ho[3,5,6], and Kin Man Yu[1,3]**

[1]Department of Physics, City University of Hong Kong, Kowloon, Hong Kong SAR
[2]Department of Physics, Khulna University of Engineering & Technology (KUET), Khulna-9203, Bangladesh
[3]Department of Materials Science and Engineering, City University of Hong Kong, Kowloon, Hong Kong SAR
[4]State Key Laboratory of Luminescence and Applications, Changchun Institute of Optics, Fine Mechanics and Physics, Chinese Academy of Sciences, Changchun 130021, China
[5] State Key Laboratory of Terahertz and Millimeter Waves, City University of Hong Kong, Kowloon, Hong Kong SAR
[6] Key Laboratory of Advanced Materials Processing & Mold (Zhengzhou University), Ministry of Education, Zhengzhou 450002, China

*Email: sujit@phy.kuet.ac.bd, kinmanyu@cityu.edu.hk

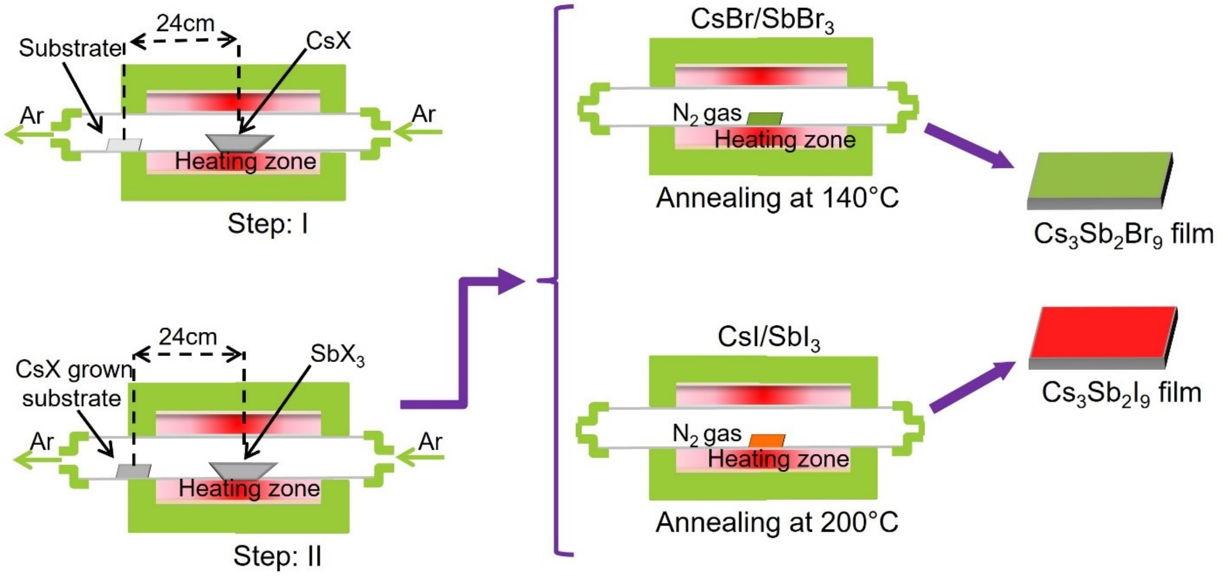

Figure S1. Schematic diagrams showing the two-step CVD process synthesis of $Cs_3Sb_2X_9$ perovskite thin films.

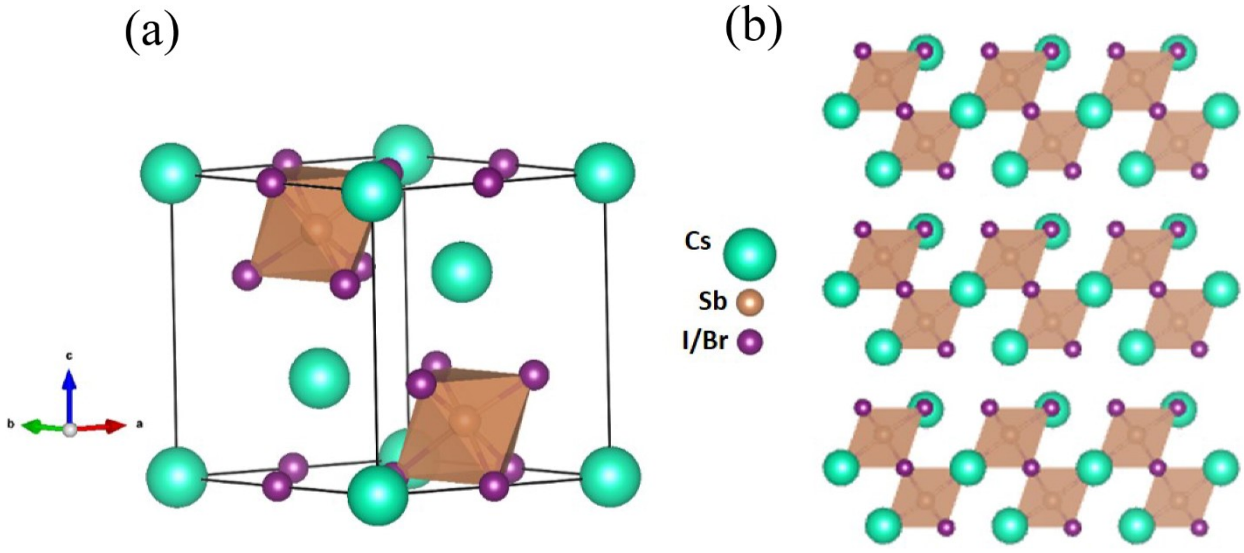

Figure S2. (a) Unit cells and (b) 2D layered structures of $Cs_3Sb_2I_9$ and $Cs_3Sb_2Br_9$ perovskite thin films.

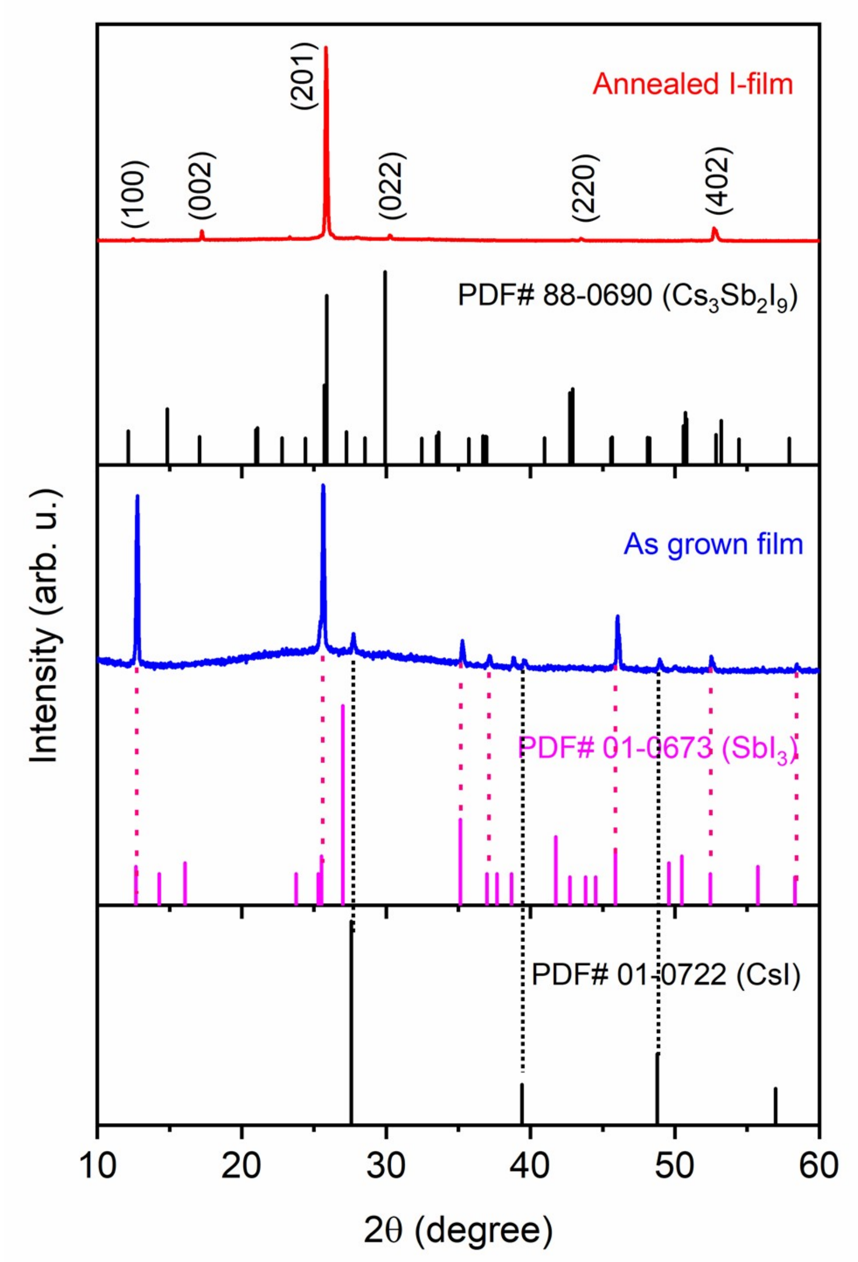

Figure S3. XRD spectra of as grown and annealed $Cs_3Sb_2I_9$ thin films.

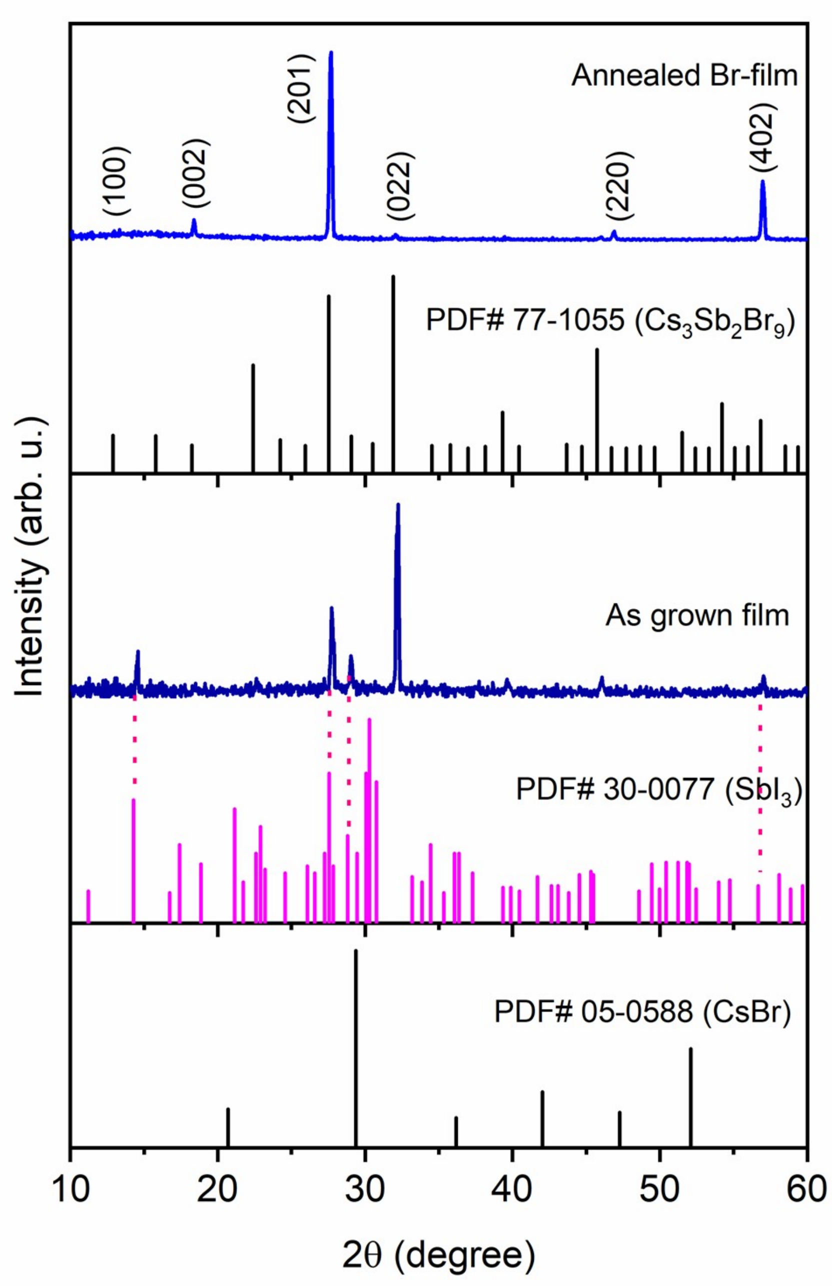

Figure S4. XRD spectra of as grown and annealed $Cs_3Sb_2I_9$ thin films.

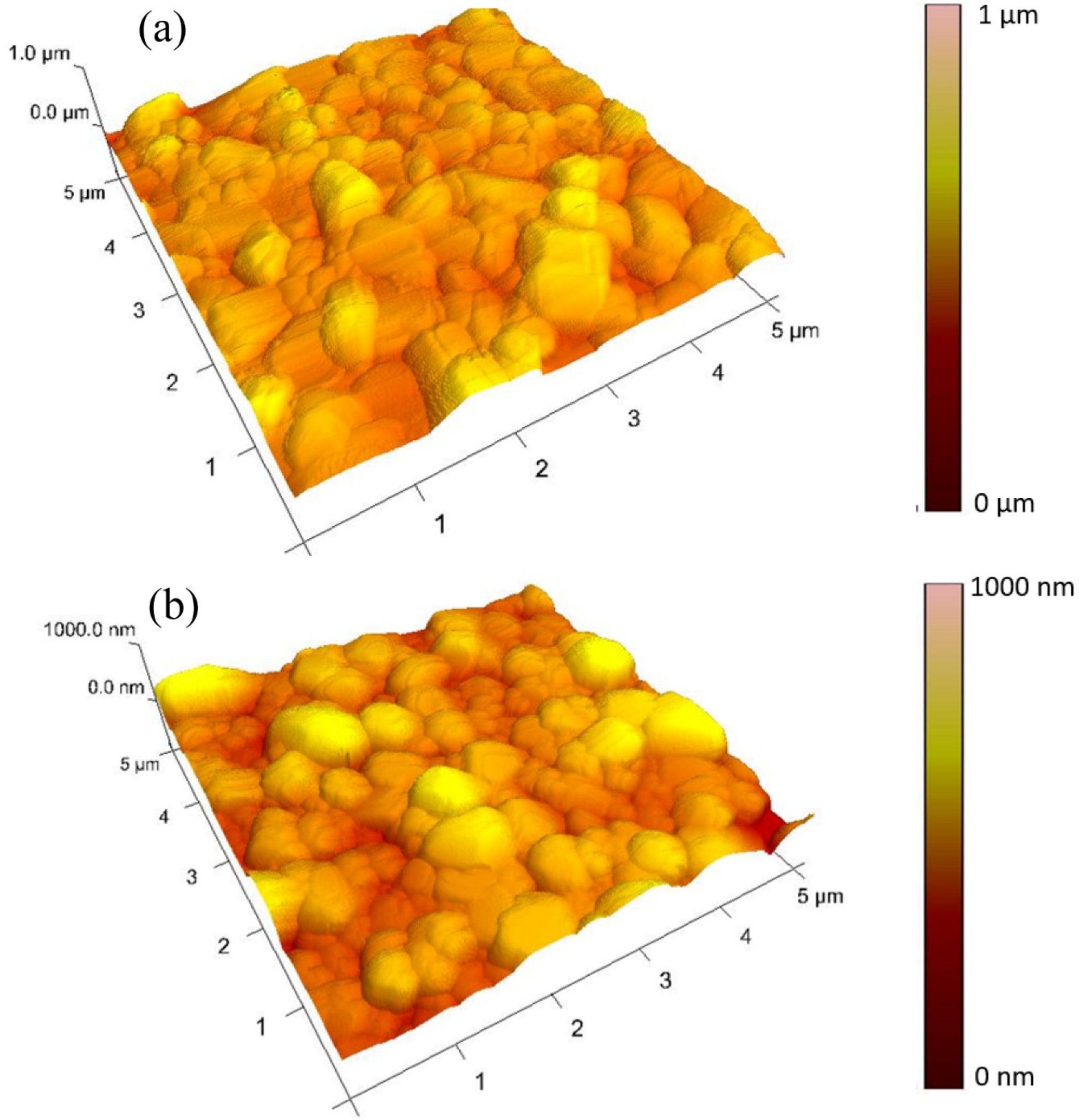

Figure S5. 3D view AFM images of (a) $Cs_3Sb_2I_9$ and (b) $Cs_3Sb_2Br_9$ perovskite thin films along with their corresponding height scale.

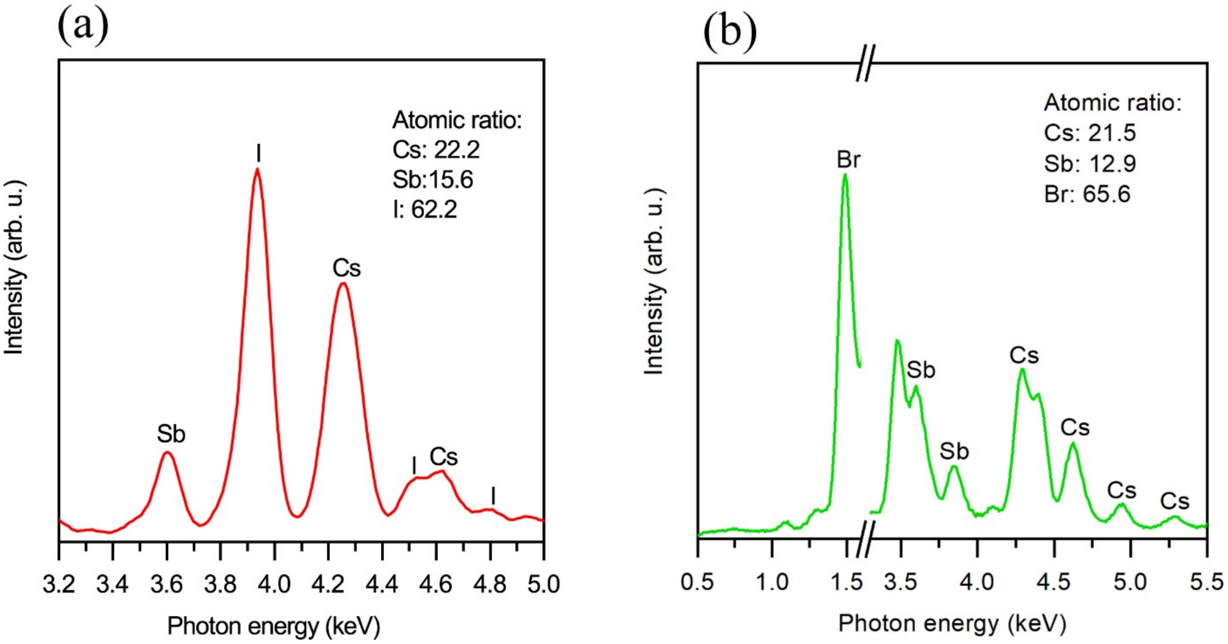

Figure S6. XRF spectra from (a) $Cs_3Sb_2I_9$ and (b) $Cs_3Sb_2Br_9$ perovskite thin films showing the atomic ratio of different elements.

The $\varepsilon_2(E)$ of an individual oscillator is expressed by[1]

$$\varepsilon_2 = \begin{cases} \frac{AE_0C(E-E_J)^2}{(E^2-E_0^2)^2+C^2E^2)}\frac{1}{E} & ; \quad (E>E_g) \\ 0 & ; \quad (E\le E_g) \end{cases} \tag{1}$$

Where A is the oscillator strength, C is a broadening parameter, E_0 is the resonance energy, and E_g is the Tauc gap (the onset of absorption). ε_1 is obtained from ε_2 by the Kramers-Krönig relations. The Tauc-Lorentz model is determined by five parameters [$\varepsilon_1(\infty)$, A, C, E_g and E_0], where $\varepsilon_1(\infty)$ is a constant which adds a high-energy contribution to ε_1.

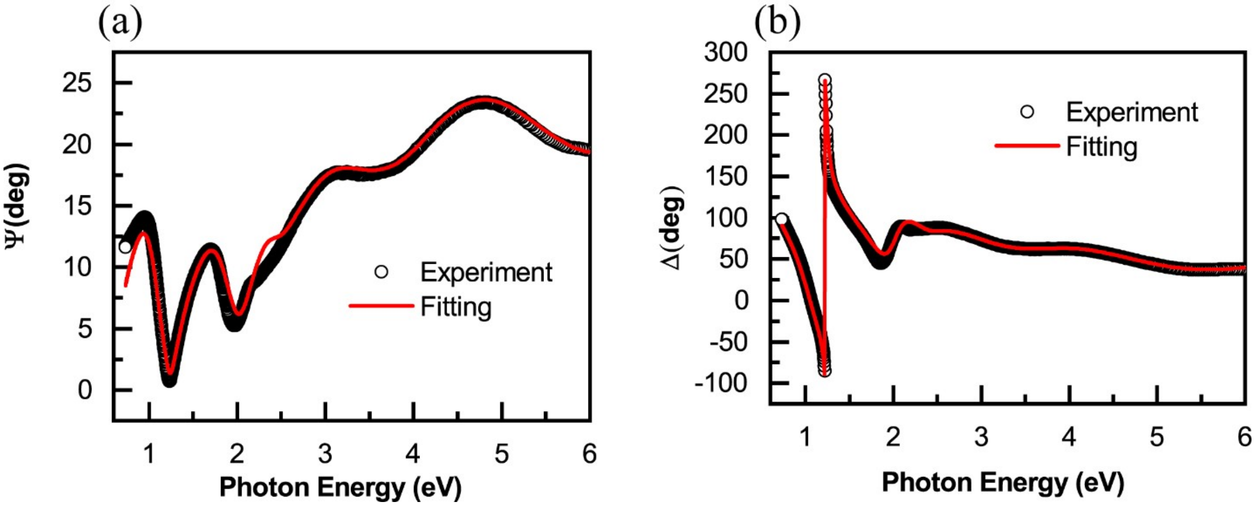

Figure S7. Ellipsometric experimental and simulated spectra (a) Psi, and (b) Delta of $Cs_3Sb_2I_9$ perovskite thin film at 65° angle of incidence.

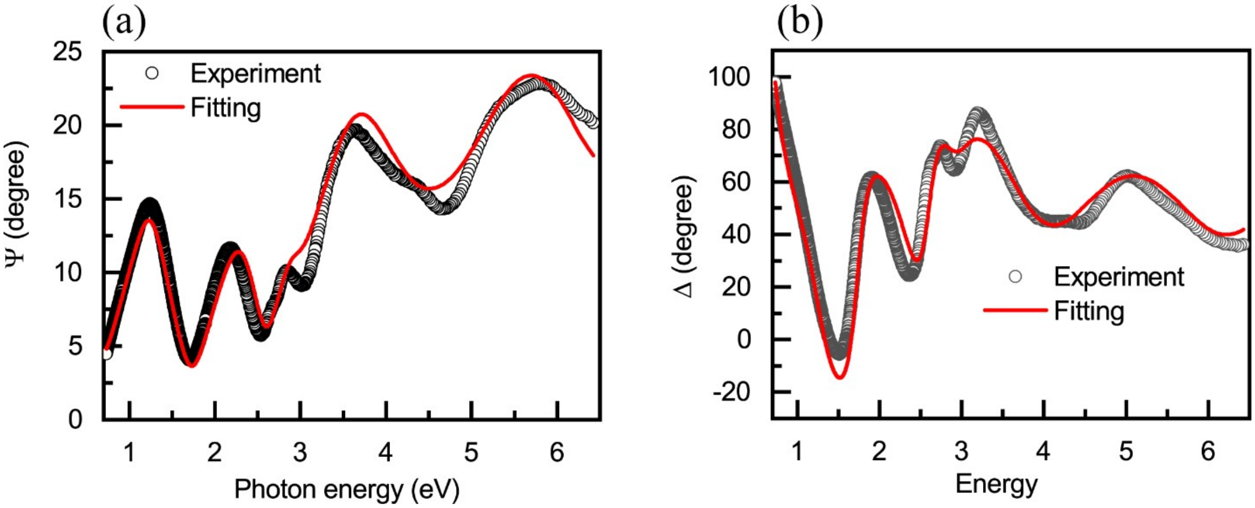

Figure S8. Ellipsometric experimental and simulated spectra (a) Psi, and (b) Delta of $Cs_3Sb_2Br_9$ perovskite thin film at 65° angle of incidence.

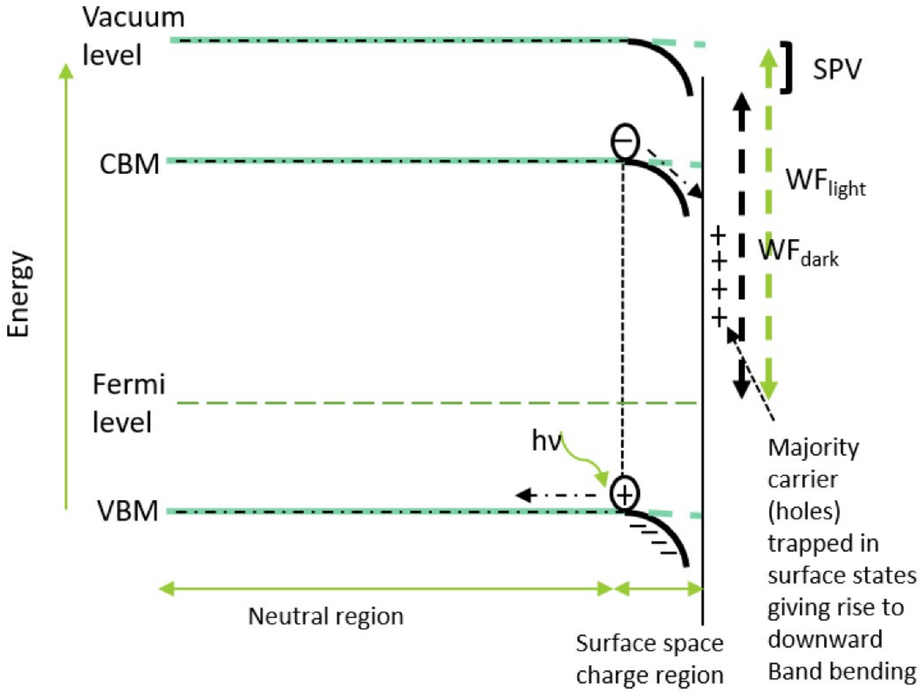

Figure S9. Schematic representation of the surface photovoltage (SPV) in a p-type semiconductor. Trapping of holes at the surface gives rise to a downward band bending. Upon illumination, the photo-generated electrons neutralize the trapped holes on the surface, thus reducing the band bending which appears as the increase in the work function. CBM- Conduction band minimum, VBM- Valence band maximum, WF- Work function.

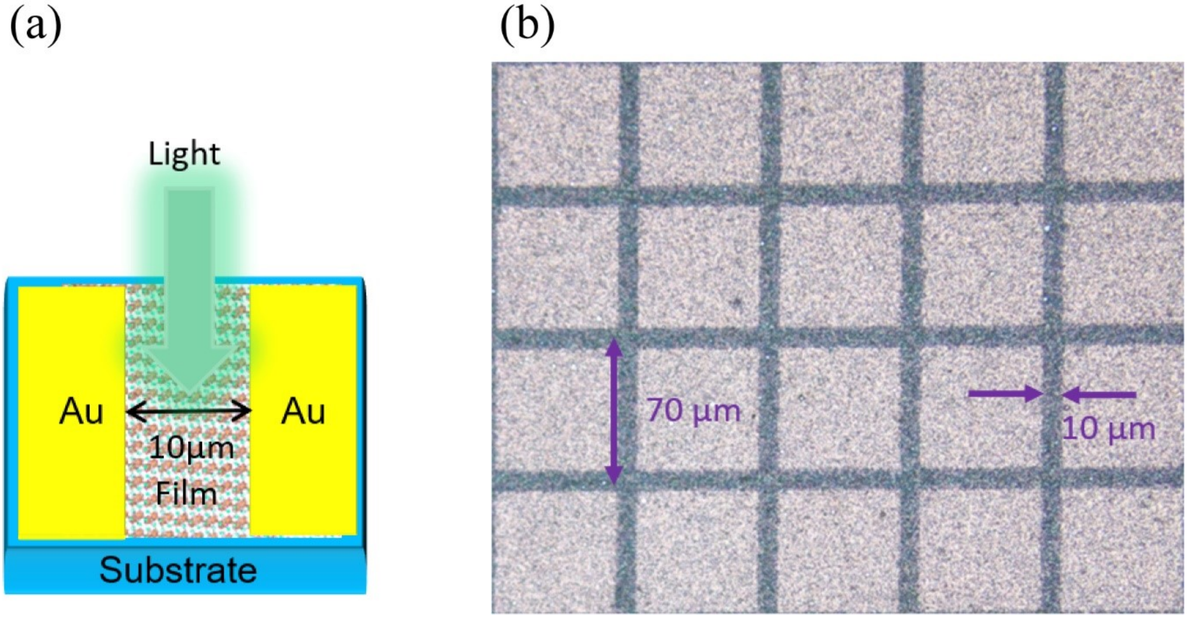

Figure S10. (a) A schematic diagram and (b) optical image of the $Cs_3Sb_2X_9$ perovskite film photodetector.

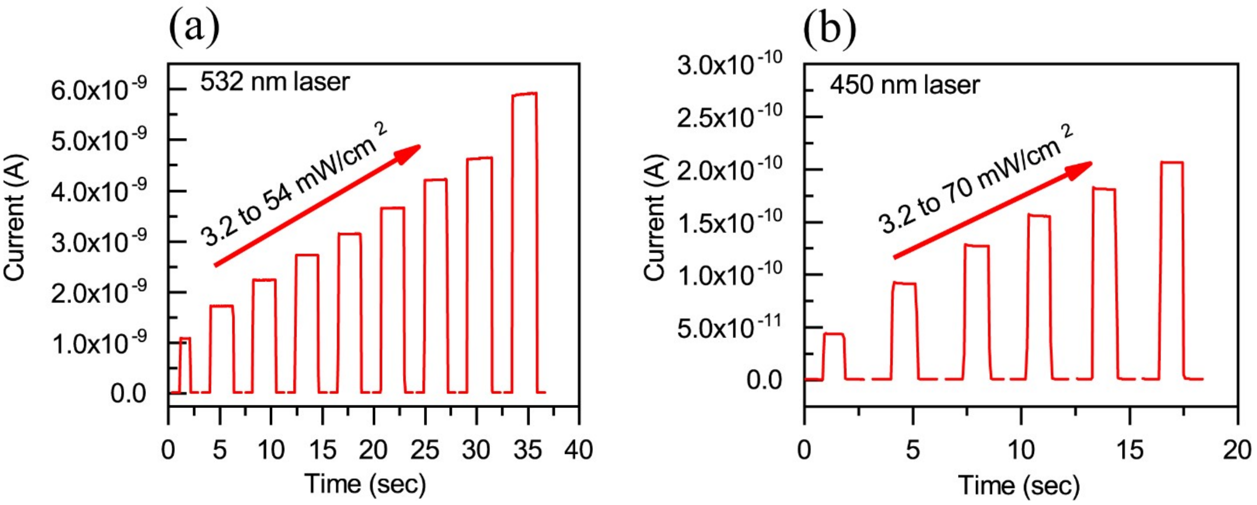

Figure S11. Photoresponse curves with different illumination power density for (a) $Cs_3Sb_2I_9$ and (b) $Cs_3Sb_2Br_9$ film photodetectors.

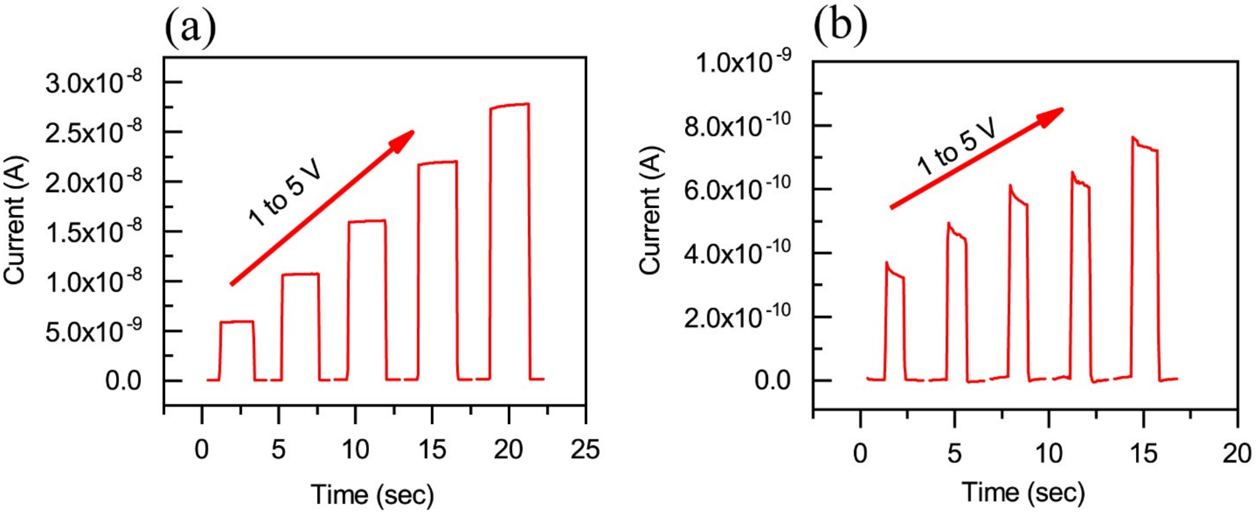

Figure S12. Photoresponse curves with different bias voltage for (a) $Cs_3Sb_2I_9$ and (b) $Cs_3Sb_2Br_9$ film photodetectors.

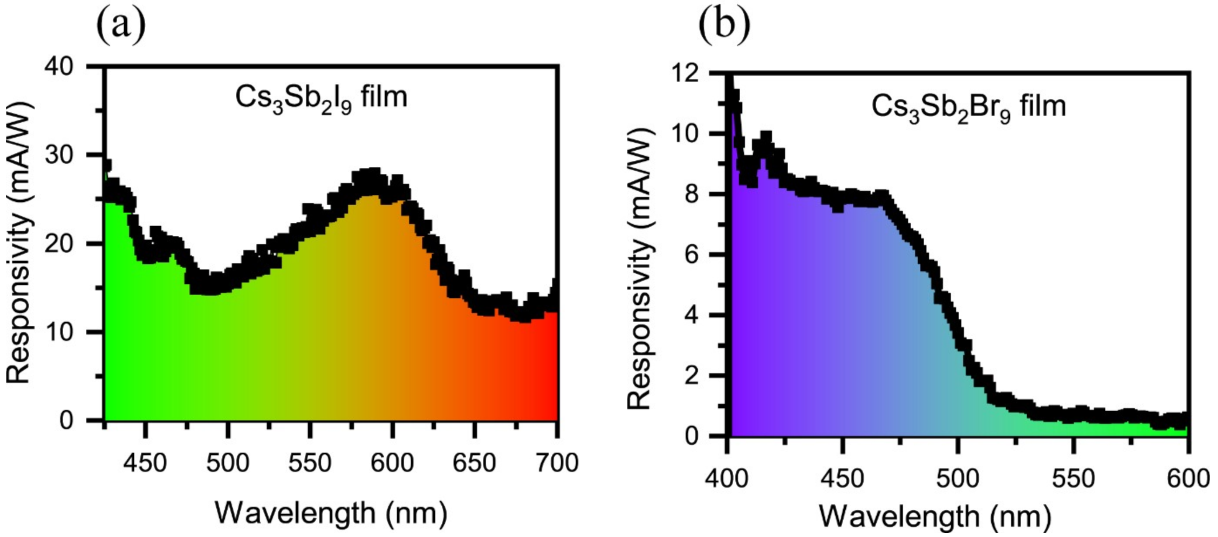

Figure S13. Wavelength dependent photoresponse of (a) $Cs_3Sb_2I_9$ and (b) $Cs_3Sb_2Br_9$ thin film photodetectors.

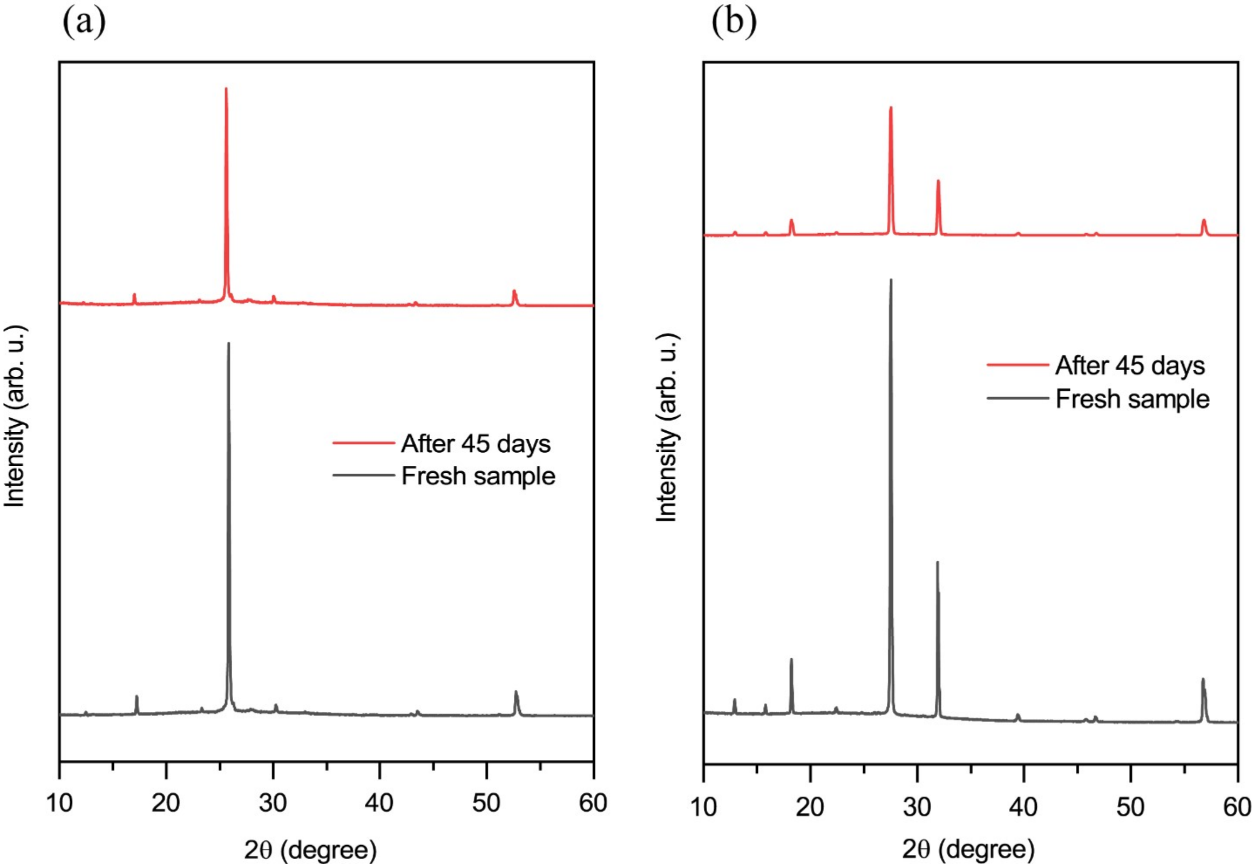

Figure S14: XRD spectra of (a) $Cs_3Sb_2I_9$ and (b) $Cs_3Sb_2Br_9$ films in fresh and after 45 days stored in ambient condition.

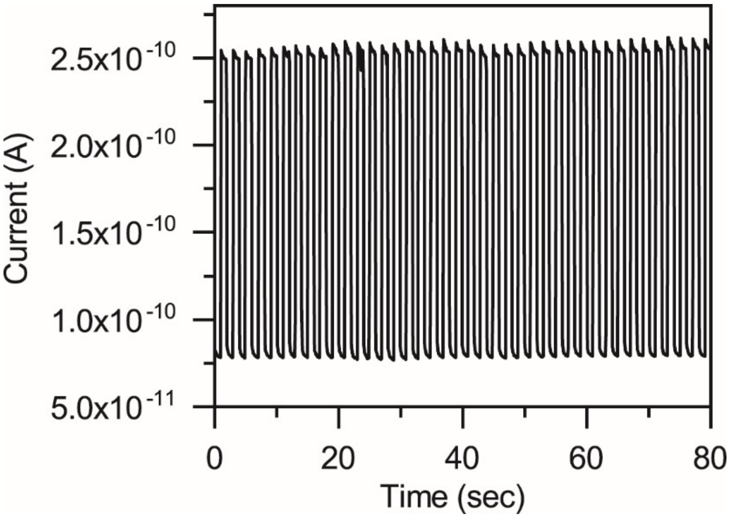

Figure S15: Reproducible on/off response of $Cs_3Sb_2I_9$ film photodetector at 1 V bias with illumination power density 54 mW/cm^2 after 45 days stored in ambient condition.

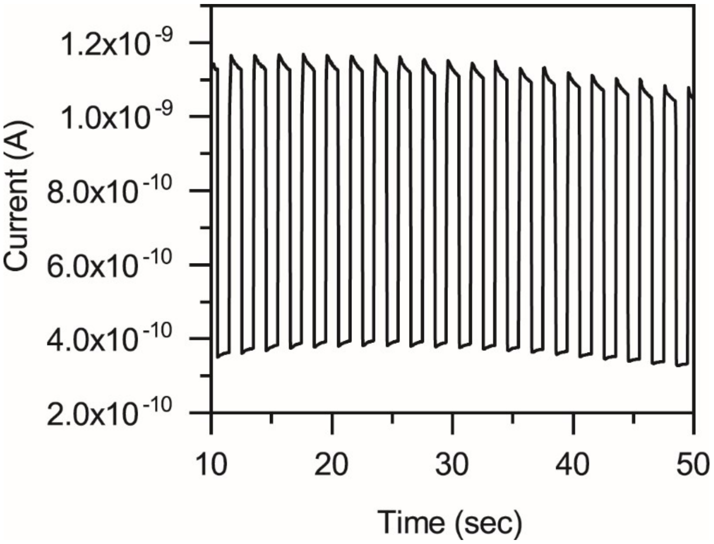

Figure S16: Reproducible on/off response of $Cs_3Sb_2Br_9$ film photodetector at 1 V bias with illumination power density 70 mW/cm^2 after 45 days stored in ambient condition.

Table S1: Comparison of the stoichiometry of $Cs_3Sb_2I_9$ films with different molar ratios

Molar ratio ($CsI:SbI_3$)	**Observed atomic percentage**	**Observed atomic ratio (Cs:Sb:I)**	**Expected atomic ratio (Cs:Sb:I)**
1:1	Cs= 26.9		

	Sb= 17.7	4.47:2.87:9	3:2:9
	I= 55.4		
1:1.5	Cs= 24.6	3.77:2.54:9	
	Sb= 16.6		
	I= 58.8		
1:2	Cs= 23.6	3.52:2.42:9	
	Sb= 16.2		
	I= 60.3		
1:3	Cs= 21.3	3:2.05:9	
	Sb= 14.6		
	I= 64.1		

REFERENCE

1 G. E. Jellison and F. A. Modine, *Appl. Phys. Lett.*, 1996, **69**, 371–373.